Title

Co-development of gut microbial metabolism and visual neural circuitry in human infants

Authors

Kevin S. Bonham
Emma T. Margolis
Guilherme Fahur Bottino
Fadheela Patel
Shelley McCann
Michal R. Zieff
Kirsty A. Donald
Laurel J. Gabard-Durnam*
Vanja Klepac-Ceraj*

ORCID numbers:

Kevin S. Bonham:	0000-0003-3200-7533
Guilherme Fahur Bottino:	0000-0003-1953-1576
Emma T. Margolis:	0000-0002-2036-8078
Fadheela Patel:	0000-0001-5177-7416
Michal Zieff:	0000-0001-9352-9947
Shelley McCann:	0000-0002-9753-7968
Kirsten A. Donald:	0000-0002-0276-9660
Laurel J. Gabard-Durnam	0000-0002-4564-8068
Vanja Klepac-Ceraj:	0000-0001-5387-5706

Running title: Infant gut microbiome associates with visual neurodevelopment

Abstract

Infancy is a time of rapid brain development supporting foundational sensory learning. The gut microbiome, also undergoing extensive developmental changes in early life, may influence brain development through metabolism of neuroactive compounds. Here, we show across the first 18 months of life that microbial genes encoding enzymes that produce and degrade neuroactive compounds, including neurotransmitters GABA and glutamate, the amino acid tryptophan, and short-chain fatty acids including acetate and butyrate, are associated with visual neurodevelopmental learning, measured by the visual-evoked potential (VEP). Microbial gene sets from stool collected around 4 months of age were strongly associated with VEP features measured from 9 to 14 months of age and showed more associations than concurrently measured gene sets, suggesting microbial metabolism in early life may have long term effects on neural plasticity and development.

Introduction

The gut microbiome in early life has potential long-term implications for brain and body health. One important way this influence can occur is through interactions with the central nervous system as a “microbial-gut-brain-axis” (Rhee, Pothoulakis, and Mayer 2009; Collins, Surette, and Bercik 2012). The metabolic potential of the microorganisms that inhabit the gut vastly exceeds that of human cells alone, with microbial genes outnumbering host genes by a hundredfold (Gilbert et al. 2018). In particular, gut microbes have the ability to metabolize and synthesize many neuroactive compounds (Valles-Colomer et al. 2019). Extensive work in preclinical models suggests that these neuroactive compounds can influence the brain through both direct and indirect routes. For example, major neurotransmitters (e.g., glutamate, γ-aminobutyric acid (GABA), serotonin, and dopamine) are readily synthesized and degraded by intestinal microbes and can directly stimulate enteric nerve cells or enter circulation and pass the blood-brain barrier to influence central nervous function (Janik et al. 2016; Ahmed et al. 2022). Glutamatergic/GABA-ergic signaling is critical for balancing the brain’s excitatory and inhibitory neurotransmission levels, and bi-directional glutamatergic/GABA-ergic signaling between the gut microbiome and brain is implicated in several physical and mental health conditions (Filpa et al. 2016; Baj et al. 2019). Similarly, the gut and the microbiome are critical to the regulation of metabolism for the neurotransmitters serotonin and dopamine, particularly through the metabolism of dietary tryptophan (Agus, Planchais, and Sokol 2018). Moreover, short-chain fatty acids (SCFAs) produced by the gut microbiome may impact the brain directly by modulating neurotrophic factors, glial and microglial maturation, and neuroinflammation (Dalile et al. 2019; Erny et al. 2021). Other indirect pathways for gut microbial influence on the brain include vagus nerve stimulation, neuroendocrine modulation and immune system regulation (Rhee, Pothoulakis, and Mayer 2009).

Rapidly growing literature connects the metabolic potential of the gut microbiome and brain function in humans (reviewed in (Ahmed et al. 2022; Parker, Fonseca, and Carding 2019; Aburto and Cryan 2024)), however, the overwhelming majority of this research is performed in adults. Importantly, both the gut microbiome and the brain undergo dramatic and rapid development over the first postnatal years (Yassour et al. 2016; Bonham et al. 2023; Lippé et al. 2007; Dean et al. 2014). However, very little is currently known about how gut-brain influences emerge or change during this critical window for both systems (Ahrens et al. 2024; Meyer et al. 2022). Interrogating this early co-development in humans is therefore key to both understanding adaptive gut-brain function and behavior and informing strategies to support it. The visual cortex has been shown to be sensitive to gut microbiome modulations in adults (Canipe, Sioda, and Cheatham 2021) and in rodents (Lupori et al. 2022), yet the visual cortex undergoes its most rapid period of plasticity and maturation over infancy when the microbiome changes most significantly (Deen et al. 2017; Ellis et al. 2021; Kiorpes 2015). Visual cortical maturation can be robustly indexed via EEG with the visual-evoked potential (VEP) response to visual stimuli from birth. The VEP is especially useful for indexing visual neurodevelopment as its morphology includes amplitude deflections and latencies to those deflections that reflect maturation of function and structure, respectively.

Here, we investigated the co-development of microbial gene functional potential - specifically genes encoding enzymes that metabolize neuroactive compounds - and visual neurodevelopment as indexed by the VEP in a longitudinal community sample of 185 infants from Gugulethu in Cape Town, South Africa recruited as part of an ongoing prospective study, called “Khula” (Zieff et al. 2024). Stool samples and EEG were collected at up to 3 visits in the first 18 months of life. Shotgun metagenomic sequencing was used to obtain microbial gene sequences from infant stool samples. To index visual cortical development, latencies and amplitudes were extracted from each deflection component of the VEP (i.e., first negative-going deflection, N1; first positive-going deflection, P1; and second negative-going deflection, N2), producing six VEP features of interest. We evaluated the concurrent association between microbial genes and VEP amplitudes and latencies and tested prospective influences of microbial genes from early visits on VEP changes at later visits to reveal the temporal dynamics of gut-brain co-development within individuals during this most critical window of plasticity.

Results

The brain and microbiome develop rapidly in the first months of life

To investigate the co-development of the gut microbiome and visual neurodevelopment, we collected stool and measured VEP in a longitudinal cohort of 194 children in South Africa in the first 18 months of life (Figure 1A, B, Table 1; visit 1, N = 119, age 3.6 ± 0.7 months, visit 2, N = 144, age 8.7 ± 1.4 months, visit 3, N = 130, age 14.2 ± 1.0 months). As expected for children at this age (Koenig et al. 2011; Yassour et al. 2016; Bäckhed et al. 2015), the microbial composition was developmentally dependent, with the first principle coordinate axis for both taxonomic profiles (Figure 1C; variance explained = 15.1%; R = -0.50)) and functional profiles (Figure 1D; variance explained = 12.9%; R = -0.57) driven strongly by the age of the subject at the time of collection. Similarly, both amplitude and latency VEP features were also strongly correlated with age, such that latencies (especially P1 and N2) became shorter, while the P1 became less positive and the N1 and 2 components became more negative in amplitude as infants got older (Figure 1E).

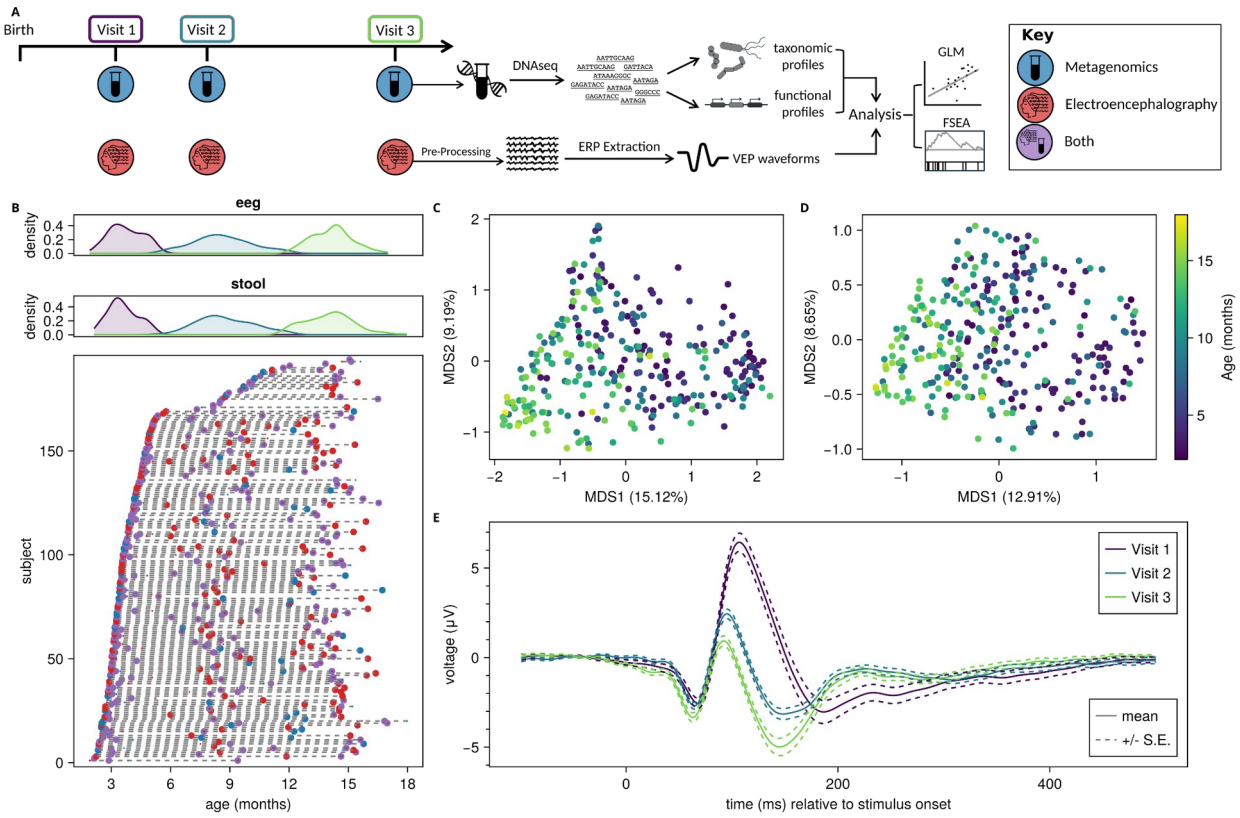

Fig. 1: The gut microbiome and VEP both develop over the first 18 months of life.
(A) Study design; participants (N=194) were seen up to 3 times over the first 18 months of life. Metagenomes and EEG data were collected, generating microbial functional profiles (stool) and VEP waveforms (EEG) used in subsequent analyses. (B) Longitudinal sampling of study participants; Density plots (top) for stool and EEG collection show the ages represented in each visit. The scatter plot (bottom) shows individual participant visits. Dotted lines connect separate visits for the same participant. When stool and EEG data were collected for the same visit (purple) but not on the same day, dot represents the median age of collection, and vertical bars in blue and red represent stool and EEG collections respectively. (C) Principal coordinate analysis (PCoA) by multidimensional scaling (MDS) on Bray-Curtis dissimilarity of taxonomic profiles; percent variance explained (fraction of positive eigenvalues) by each of the first two axes are indicated on the x and y axes respectively. (D) PCoA of microbial functional profiles (UniRef90s). (E) Average VEP waveforms at each visit.

Microbial genes with neuroactive potential are associated with visual development

To test whether microbial metabolic potential was related to early life brain activity, we performed feature set enrichment analysis (FSEA) using groups of potentially neuroactive microbial genes and the VEP amplitude and latency features (Bonham et al. 2023; Valles-Colomer et al. 2019). For each gene set that had at least 5 genes represented in a given comparison group, logistic regression was performed using VEP features as predictors and the presence or absence of each microbial gene in the metagenome as the response to determine concurrent associations (see Methods). Z statistics for in-set genes were compared to all genes

using a permutation test to determine significance of the associations as described in (Subramanian et al. 2005). Of the 35 genesets assessed, 19 had sufficient representation to test, and of those, 18 were significantly associated with at least one EEG feature during at least one visit within the 18-month window after correcting for false discovery rate (Benjamini-Hochberg, q < 0.2; Figure 2, Table 2). Microbial genes involved in synthesis or degradation of molecules with neuroactive potential were associated with both VEP amplitudes or latencies at each visit, demonstrating widespread associations between early life gut microbiome and visual cortex neurodevelopment. The number of these associations increased over time (visit 1 had 6 associations, visit 2 had 24, and visit 3 had 37), which could reflect the fact that *in utero* development is thought to occur in a sterile environment, providing less opportunity for microbial metabolism to influence visual cortex development in the first 3 months of life.

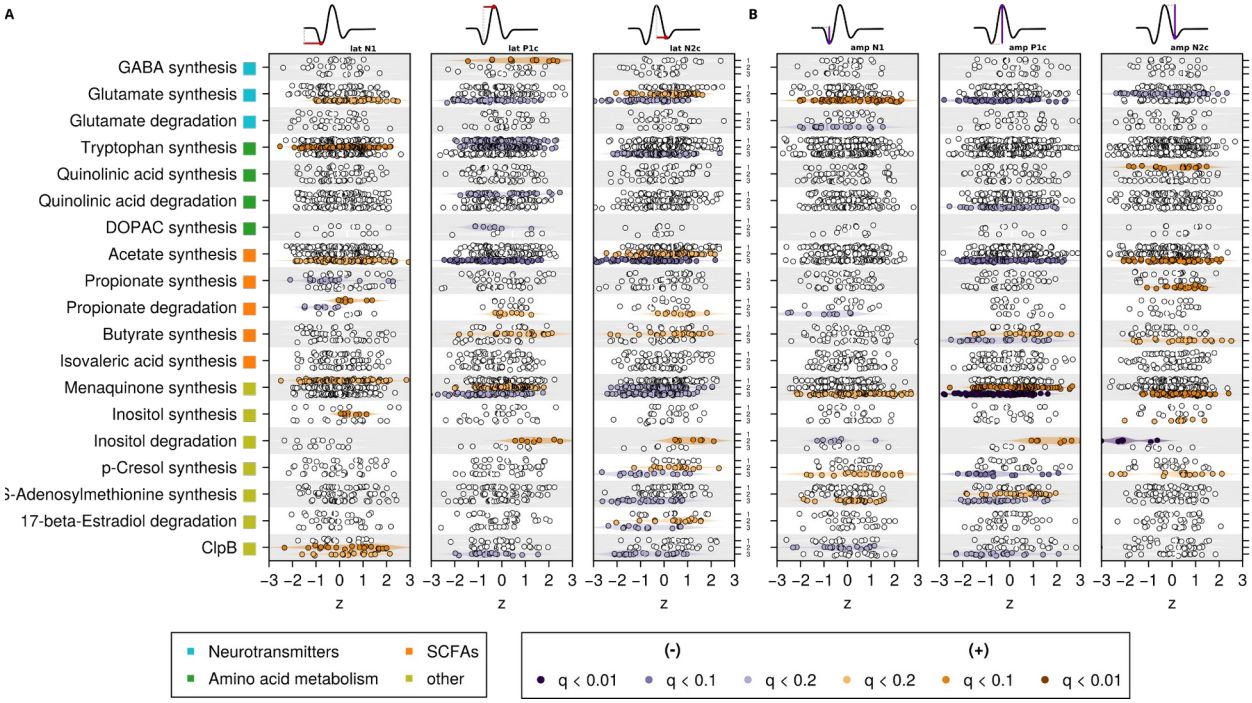

Fig. 2: Concurrent feature set enrichment analysis of microbial neuroactive genes and VEP for three visits.

FSEA results for all genesets where at least one visit had a significant hit (q < 0.2) with at least one VEP latency (A) or amplitude (B). Dots indicate the Z-statistic from logistic regression for each gene in a gene set. Vertical bars indicate the median Z-statistic for the gene set as a whole. Y-axis position for each gene set indicates visit number. Visit 1 for inositol degradation and DOPAC synthesis were not tested, since there were fewer than 5 genes from those genesets present in the sample (See Methods).

Specifically, across the gene sets involved in neurotransmitter synthesis and degradation, glutamate synthesis showed robust associations with all VEP features, primarily at the 3rd visit (mean age 14.3 months), while glutamate degradation was weakly but significantly associated only with the amplitude of N2 at visit 3. GABA synthesis was also associated with the latency of the P1 peak at visit 1 (mean age 3.6 months). The regulation of this balance between glutamate and GABA (i.e., excitatory/inhibitory balance) is important for modulating neuroplasticity in the visual cortex during infancy (Fagiolini and Hensch 2000; Hensch et al. 1998), and suggests that microbial metabolism is related to the VEP as an index of this changing neuroplasticity. Gene

sets involved in tryptophan metabolism, which is linked to the metabolism of the neurotransmitter serotonin as well as other neuroactive molecules such as kynurenine (Agus, Planchais, and Sokol 2018) was associated with VEP latencies of P1 at visit 1, N1 and P1 at visit 2, and N2 at visit 3. The degradation of quinolinic acid, also downstream of tryptophan metabolism, was negatively enriched in children with shorter P1 latency at visit 1 and smaller P1 amplitude at visit 3, while the synthesis of quinolinic acid was positively associated with the amplitude of the N2 peak at visit 1. Serotonin is a key regulator of other neurotransmitters, while quinolinic acid is part of the kynurenine pathway and is a neurotoxin that can cause neuronal dysfunction, but may also play a role in glutamate uptake in the brain (Lugo-Huitrón et al. 2013; Tavares et al. 2000).

Amongst the short-chain fatty acid (SCFA) metabolizing gene sets tested, acetate synthesis was strongly associated with all VEP features except N1 amplitude at visit 3, and also with N2 latency at visit 2. Propionate degradation was significantly associated with VEP latencies at every visit over the 18-month window (N1 at visits 1 and 2, and both P1 and N2 at visit 3), as well as with the amplitude of N1 at visit 3, while propionate synthesis was negatively associated with N1 latency at visit 1 and positively associated with N2 amplitude at visit 3. Butyrate synthesis is also associated with P1 and N2 latencies at visit 2, and with their amplitudes at visit 3. SCFAs play important roles in immune regulation, including neuroinflammation. Propionate is widely regarded as neuroprotective, having indirect effects on the CNS by regulating inflammatory responses and stimulating the release of GLP-1 from neuroendocrine cells in the gut epithelium, while circulating butyrate increases myelination (Chen et al. 2019) . Finally, within the remaining gene sets tested, we observed robust associations in particular between menaquinone (Vitamin K2) gene sets and the VEP features over this infancy window. This is reassuring as vitamin K2 specifically is posited to promote healthy vision both outside of the brain through effects on the retina and within the brain where it can protect neural circuits from oxidative stress (Li et al. 2003). Notably, across significant gene set associations with VEP features, the P1 and N2 component amplitudes and latencies were consistently the most sensitive to these microbial gene sets. Both P1 and N2 components are known to show the most dramatic changes with development during the first year of life and may best reflect underlying visual learning and plasticity at this stage.

Microbial metabolic potential predicts future brain development in infancy

Given that differences in metabolic potential of the early life microbiome may exert their effects over time, we sought to determine whether microbial genes at early time points were associated with subsequent VEP development. To investigate this, we performed FSEA on stool samples collected at visit 1 with VEP measured at visit 2 (age at stool collection = 3.6 ± 0.8 months, age at VEP = 8.6 ± 1.5 months) or visit 3 (age at stool collection = 3.7 ± 0.7 months, age at VEP = 14.1 ± 1.1 months), as well as visit 2 stool samples with visit 3 VEP (age at stool collection = 8.9 ± 1.5 months, age at VEP = 14.3 ± 1.0 months) (Figure 3A). All gene sets except DOPAC synthesis that had a significant hit with concurrently measured VEP were also significantly associated with at least one future VEP feature (Figure 3B, Tables 2-5). Notably, the quantity of those associations increased substantially for all longitudinal comparisons compared to concurrent ones. For example, only 6 microbial gene sets were associated with visit 1 VEP, and

each of those was only associated with a single concurrently measured VEP feature. By contrast, 13 visit 1 gene sets were associated with visit 2 VEP features, and 11 were associated with visit 3 VEP features, the majority (9/13 for visit 2, 8/11 for visit 3) were associated with at least 2 VEP features, and nearly half (6/13 for visit 2, 5/11 for visit 3) were associated with more than 2.

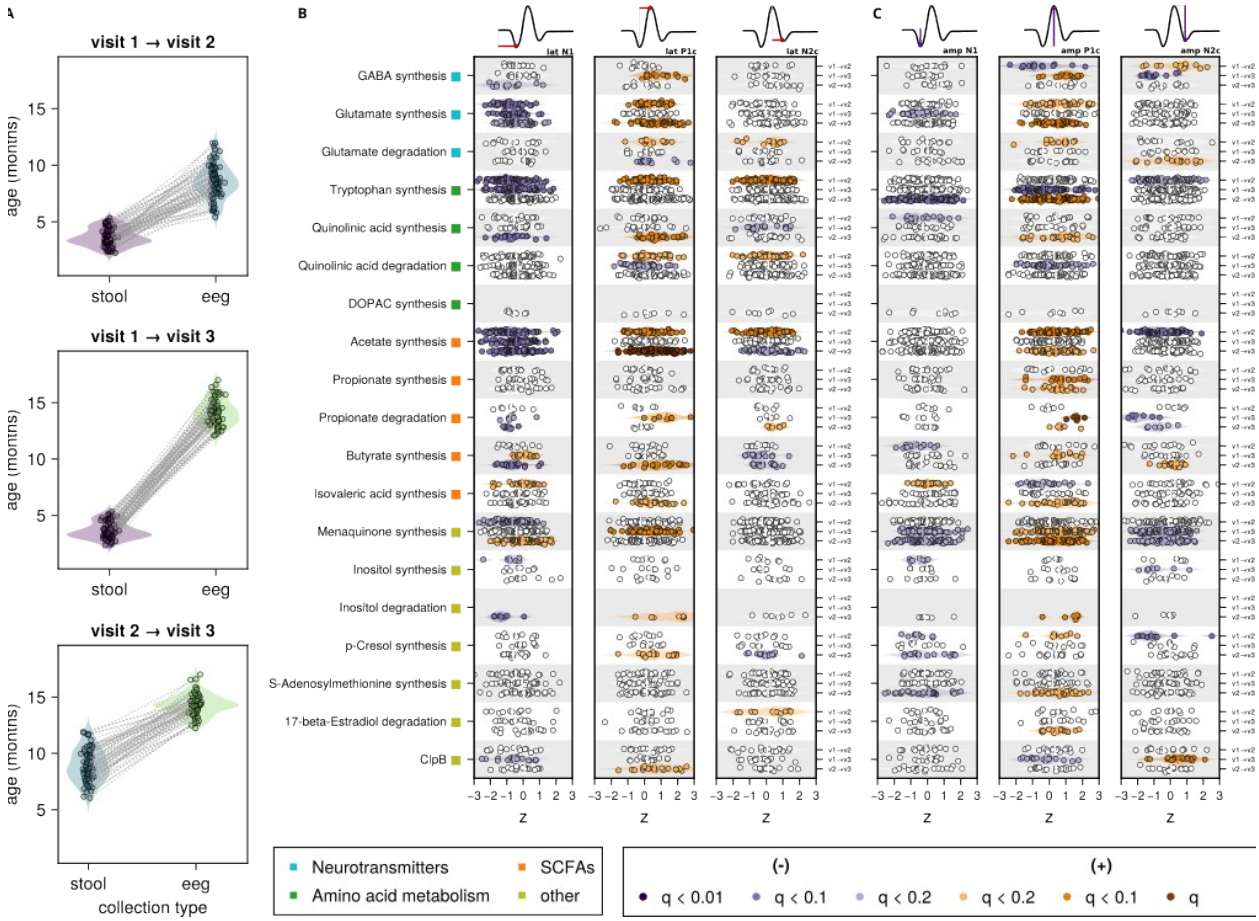

Fig. 3: Gut microbial genes predict future VEP latencies and amplitudes

(A) Age distributions for stool samples (left) and VEP (right) for each longitudinal comparison (same individual) tested, V1 stool Z→V2 VEP, V1 stool →V3 VEP, and V2 stool →V3 VEP. As in Figure 2, (B) and (C) show FSEA results for all genesets where at least one visit had a significant hit ($q < 0.2$) with at least one VEP latency or amplitude respectively. Dots indicate the Z-statistic from logistic regression for each gene in a gene set. Vertical bars indicate the median Z-statistic for the gene set as a whole. The Y-axis position for each gene set indicates longitudinal comparison. V1 → V2 and V1 → 3 for inositol degradation and DOPAC synthesis were not tested, since there were fewer than 5 genes from those genesets present in the sample (See Methods).

224 **Table 2: Longitudinal FSEA, visit 1 stool -> visit 2 VEP**
225

Gene set	Feature type	Peak	Enrichment	Q value
GABA synthesis	amp	P1	-0.3987298838	0.08078918919
		N2	0.3661036051	0.1129448276
Glutamate synthesis	latency	N1	-0.2829156583	0.04452
		P1	0.2625066112	0.08078918919
	amp	P1	0.2316538042	0.1023130435
Glutamate degradation	latency	P1	0.3369665011	0.1598153846
		N2	0.3252682367	0.1800808989
	amp	P1	0.3256631998	0.1760093023
Tryptophan synthesis	latency	N1	-0.2211303459	0.02725714286
		P1	0.1671470069	0.08078918919
		N2	0.1900183195	0.04845714286
	amp	N2	-0.1630723325	0.1023130435
Quinolinic acid synthesis	amp	N1	-0.2735268422	0.1609156627
Quinolinic acid degradation	latency	P1	0.1979735587	0.1023130435
		N2	0.1950682309	0.1118888889
Acetate synthesis	latency	N1	-0.2190895918	0.02935384615
		P1	0.1926523891	0.06115384615
		N2	0.2157444594	0.0318
	amp	P1	0.1860132394	0.0742
		N2	-0.1960332174	0.05492727273
Butyrate synthesis	amp	N1	-0.3193476197	0.1698494118
Isovaleric acid synthesis	latency	N1	0.2711007176	0.1223076923
	amp	N1	0.2412188311	0.1800808989
		P1	-0.2409522895	0.1609156627
Menaquinone synthesis	latency	N1	-0.1393490274	0.1598153846
Inositol synthesis	amp	N1	-0.4295268274	0.1804304348
	latency	N1	-0.4219126859	0.1834357895
p-Cresol synthesis	amp	N1	-0.3665789266	0.1825935484
		P1	0.452086746	0.1014571429
		N2	-0.5164507055	0.04452
17-beta-Estradiol degradation	latency	N2	0.3550449716	0.1800808989

226
227
228

Table 3: Longitudinal FSEA, visit 1 stool -> visit 3 VEP

Gene set	Feature type	Peak	Enrichment	Q value
GABA synthesis	latency	P1	0.4343386934	0.04452
	amp	P1	0.4099001639	0.0742
		N2	-0.5065759161	0.02544
Glutamate synthesis	latency	N1	-0.3035011084	0.02935384615
	amp	N1	-0.2344054782	0.1118888889
Tryptophan synthesis	latency	N1	-0.1875306139	0.04452
	amp	P1	-0.2176124281	0.0159
Quinolinic acid degradation	latency	P1	-0.1862809727	0.109392
		N2	-0.2624478514	0.1834357895
	amp	P1	-0.1689430121	0.1609156627
Acetate synthesis	latency	N1	-0.1728769986	0.08078918919
Propionate synthesis	amp	P1	0.3586598762	0.08078918919
Propionate degradation	latency	N1	-0.5097549612	0.109392
		P1	0.5345516637	0.08806153846
	amp	P1	0.738806805	0
		N2	-0.6669122013	0.02725714286
Butyrate synthesis	latency	N1	0.3373261944	0.1223076923
		N2	-0.3232764867	0.1498520548
	amp	P1	0.368868764	0.1014571429
Menaquinone synthesis	latency	P1	0.1582676302	0.08703157895
	amp	N1	-0.1417486481	0.1397408451
		P1	0.1488038682	0.1131864407
		N2	-0.1567020165	0.1023130435
Inositol synthesis	amp	N2	-0.4538038427	0.1210451613
ClpB	latency	N1	-0.2835050435	0.1804304348
	amp	P1	-0.3284206328	0.1129448276
		N2	0.3585858703	0.08001290323

232 **Table 4: Longitudinal FSEA, visit 2 stool -> visit 3 VEP**

233

Gene set	Feature type	Peak	Enrichment	Q value
GABA synthesis	latency	N1	-0.3762158971	0.107325
Glutamate synthesis	latency	N1	-0.1676219701	0.1609156627
		P1	0.2979689116	0.0159
	amp	P1	0.23424529	0.03816
Glutamate degradation	latency	P1	0.3174180129	0.14045
	amp	N2	0.2829464416	0.187555102
Tryptophan synthesis	amp	N1	-0.1554890366	0.06083478261
		P1	0.1865391121	0.02935384615
Quinolinic acid synthesis	latency	N1	-0.3186382801	0.061056
		P1	0.333137823	0.043725
	amp	P1	0.2577611214	0.1391826087
Acetate synthesis	latency	N1	-0.1673242602	0.061056
		P1	0.2574696731	0
		N2	-0.1373776916	0.1529837838
	amp	P1	0.1469554921	0.1210451613
Propionate synthesis	amp	P1	0.2994151994	0.1262363636
Propionate degradation	latency	N1	-0.5503973578	0.0742
		N2	0.4492537427	0.1609156627
	amp	P1	0.5088146404	0.1118888889
		N2	-0.4229989983	0.187555102
Butyrate synthesis	latency	N1	-0.3316428446	0.08078918919
		P1	0.3335618515	0.0742
		N2	-0.2908124776	0.1223076923
	amp	N2	0.3066681625	0.1118888889
Isovaleric acid synthesis	latency	P1	0.2316852688	0.1556526316
	amp	P1	0.2469367892	0.1129448276
Menaquinone synthesis	latency	N1	0.1528795641	0.1210451613
	amp	N1	-0.1644331641	0.107325
		P1	0.2014568364	0.02935384615
		N2	-0.1634034966	0.1121672727
Inositol degradation	latency	N1	-0.6381259915	0.02935384615
		P1	0.5323381792	0.1014571429

	amp	P1	0.6413929993	0.02935384615
p-Cresol synthesis	latency	P1	0.3118799423	0.1397408451
		N2	-0.3152864697	0.1391826087
	amp	N1	-0.3039764673	0.1658142857
S-Adenosylmethionine synthesis	amp	N1	-0.2228894468	0.1556526316
		P1	0.2295724682	0.1347940299
17-beta-Estradiol degradation	amp	P1	0.2818613888	0.187555102
ClpB	latency	P1	0.2687857561	0.1804304348

Neurotransmitters GABA and glutamate, tryptophan metabolism (tryptophan and quinolinic acid) and SCFAs including menaquinone and acetate were all significantly associated with multiple VEP features across multiple longitudinal comparisons.

Discussion

The past decade has seen a remarkable growth in our understanding of the relationships between the gut microbiome and the brain. However, a great deal of that investigation has focused on neuropsychiatric disorders or atypical development, and animal models of those disorders (e.g., autism spectrum disorder, depression/anxiety) have an unknown relationship to the human disorders that they represent, limiting their explanatory potential. A research program that investigates typical development using non-invasive measurements in humans, that is accurate and reproducible and shows variation in the first year of life, and that is directly measurable in rodent models is sorely needed. The relationship between gut microbial metabolism and VEP development offers just such a paradigm.

Here, we have shown a robust, prospective relationship between microbial genes involved in the metabolism of neuroactive compounds and the development of visual response in the brain as measured by EEG. It is particularly encouraging that the microbial metabolism earlier in life is more strongly associated with future measures of VEP than those collected concurrently. While not dispositive, this would be the predicted outcome if microbial genes are causally influencing brain development. It is also encouraging that the gene sets most associated with VEP development are for the metabolism of molecules with known links to developmental neuroplasticity and development of the visual cortex (Fagiolini and Hensch 2000; Hensch et al. 1998; Takesian et al. 2018).

Interestingly, the sign of several associations changes from one comparison to another. For example, acetate synthesis, tryptophan synthesis, and quinolinic acid degradation are all positively associated with N2 latency when comparing visit 1 stool to visit 2 VEP, but negatively associated when comparing visit 2 stool to visit 3 VEP. The sign of tryptophan synthesis associations is particularly unstable; it is positively associated with P1 latency when comparing visit 1 or visit 2 stool to the following visit VEP, but negatively associated when comparing visit 1 stool to visit 3 VEP, is negatively associated with P1 amplitude and N2 amplitude in one

comparison but positively associated in another. These results suggest that the impact of microbial metabolism on brain development may be context dependent.

One limitation of this study is the fact that we are only able to observe the genomic composition of the microbiome, rather than the concentration of metabolites themselves. This prevents us from determining the concentration of these molecules in the gastrointestinal tract, blood, and brain, as the abundance of these genes does provide information about their activity, their interactions with other metabolic pathways (including those of the host), or absorption by colonic epithelial cells. Additionally, the relationship between gene abundance and molecule concentration may be counterintuitive. For example, genes for breaking down a molecule may be prevalent if that molecule is at high concentrations, or the molecules may be rapidly degraded by other members of the community the moment they are produced. The balance of degradation and synthesis occurs both at the individual organism level and at the community level. This may also explain the somewhat puzzling results where some gene set / VEP feature associations change from positive to negative association (or vice versa) when comparing different timepoints. It may be that the relationship between metabolite and brain development remains the same, while the relationship between molecules and microbial selection changes at different stages of life. Addressing these limitations in humans is challenging, even if looking at stool metabolites, since overall exposure throughout the gastrointestinal tract is not necessarily reflected in the final concentration of those molecules in stool. Therefore, metabolites from blood plasma could provide more accurate systemic concentrations of molecules, but challenges remain on how to interpret them (Deng et al. 2023; Dekkers et al. 2022).

Given that the VEP is evolutionarily conserved in mammals and can be accurately measured during rodent development, the hypotheses generated in humans in this study are readily testable using *in vivo* models. Germ free or defined-microbiome animals (Wymore Brand et al. 2015; Kennedy, King, and Baldridge 2018) may be supplemented with specific molecules such as SCFAs, or colonized with microbial species lacking or providing specific metabolic pathways, and molecule concentrations in tissues from the gut to the brain can be directly assessed. Uncovering relationships between microbial metabolism and specific molecules may also generate hypotheses that can be confirmed in human data. This study provides a foundation for deep investigation of the relationships between the gut microbiome and brain development.

Materials and methods

Cohort, ethics, etc

Participants and Study Design

Infants were recruited from local community clinics in Gugulethu, an informal settlement, in Cape Town, South Africa as part of an ongoing longitudinal study (most of the enrollment happened prenatally with 39% of infants enrolled shortly after birth (Zieff et al. 2024)). The first language for the majority of residents in this area is Xhosa. Study procedures were offered in English or Xhosa depending on the language preference of the mother. This study was approved by the relevant

university Health Research Ethics Committees (University of Cape Town study number: 666/2021). Informed consent was collected from mothers on behalf of themself and their infants. Demographic information including maternal place of birth, primary spoken language, maternal age at enrollment, maternal educational attainment, and maternal income were collected at enrollment (see Table 1).

Families were invited to participate in three in-lab study visits over their infant's first year and a half of life. At the first in-lab study visit (hereafter Visit 1), occurring when infants were between approximately 2 months and 6 months of age, the following data were collected: the infants' age (in months), sex, infant electroencephalography (EEG), and infant stool samples.

At the second study visit (hereafter Visit 2), occurring when infants were between approximately 6 months and 12 months of age (age in months: *M*=8.60, SD=1.48, range=5.41-12.00) and at the third study visit (hereafter Visit 3), occurring when infants were between approximately 12 months and 17 months of age (age in months: *M*=14.10, SD=1.04, range=12.10-17.00), infant EEG and stool samples were collected again. At visits in which infants were unable to complete both EEG and stool samples on the same day, EEG and stool samples were collected on different days. For concurrent time point analyses, infants with EEG and stool collected more than two months apart were excluded. Not all infants had EEG and microbiome data collected at all three timepoints or contributed usable data at all three timepoints.

All enrolled infants received a comprehensive medical exam at each visit, which included assessments of eye-related conditions. Several infants (n=3) were identified as having eye-related anomalies during the medical exam, and they were excluded from any further analyses.

EEG Processing

EEG Data Acquisition

Electroencephalography (EEG) data were acquired from infants while they were seated in their caregiver's lap in a dimly-lit, quiet room using a 128-channel high density HydroCel Geodesic Sensor Net (EGI, Eugene, OR), amplified with a NetAmps 400 high-input amplifier, and recorded via an Electrical Geodesics, Inc. (EGI, Eugene, OR) system with a 1000 Hz sampling rate. EEG data were online referenced to the vertex (channel Cz) through the EGI Netstation software. Impedances were kept below 100KΩ in accordance with the impedance capabilities of the high-impedance amplifiers. Geodesic Sensor Nets with modified tall pedestals designed for improving inclusion of infants with thick/curly/tall hair were used as needed across participants (Mlandu et al., 2024). Shea moisture leave-in castor oil conditioner was applied to hair across the scalp prior to net placement to improve both impedances and participant comfort (Mlandu et al., 2024). This leave-in conditioner contains insulating ingredients so there is no risk of electrical bridging and has not been found to disrupt the EEG signal during testing (unpublished data). Conditioning hair in this way allows for nets to lay closer to the scalp for curly/coily hair types and makes for far more comfortable net removal at the end of testing.

The Visual-Evoked Potential (VEP) task was presented using Eprime 3.0 software (Psychology Software Tools, Pittsburgh, PA) on a Lenovo desktop computer with an external monitor 19.5 inches on the diagonal facing the infant (with monitor approximately 65 cm away from the infant). A standard phase-reversal VEP was induced with a black and white checkerboard (1cm x 1 cm squares within the board) stimulus that alternated presentation (black squares became white, white squares became black) every 500 milliseconds for a total of 100 trials. Participant looking was monitored by video and by an assistant throughout data collection. If the participant looked away during the VEP task, the task was rerun.

EEG Data Pre-Processing

VEP data were exported from native Netstation .mff format to .raw format and then pre-processed using the HAPPE+ER pipeline within the HAPPE v3.3 software, an automated open-source EEG processing software validated for infant data (Monachino et al. 2022). A subset of the 128 channels were selected for pre-processing that excluded the rim electrodes as these are typically artifact-laden. The HAPPE pre-processing pipeline was run with user-selected specifications.

Pre-processed VEP data were considered usable and moved forward to VEP extraction if HAPPE pre-processing ran successfully, at least 15 trials were retained following bad trial rejection, and at least one good channel was kept within the visual ROI. Note that channels marked bad during pre-processing had their data interpolated as part of standard pre-processing pipelines for ERPs (Monachino et al. 2022). Interpolated channels were included in analyses here as is typically done in developmental samples and given the low overall rates of interpolation present (e.g., all groups at all visits had an average of between 4 to 5 of 5 possible good channels in the region of interest retained).

Visual-Evoked Potentials (VEPs)

VEP waveforms were extracted and quantified using the HAPPE+ER v3.3 GenerateERPs script (Monachino et al. 2022). Electrodes in the occipital region were selected as a region of interest (i.e., E70, E71, E75, E76, E83). The VEP waveform has three main components to be quantified: a negative N1 peak, a positive P1 peak, and a negative N2 peak. Due to normative maturation of the waveforms as infants age, one set of user-specified windows for calculating component features was used for Visit 1 and 2 and another was used for Visit 3. For Visits 1 and 2, the window for calculating features for the N1 component was 40-100 ms, 75-175 ms for the P1 component, and 100-325 ms for the N2 component. For Visit 3, the window for calculating features for the N1 component was 35-80 ms, 75-130 ms for the P1 component, and 100-275 ms for the N2 component.

To correct for the potential influence of earlier components on later components, corrected amplitudes and latencies were calculated and used in all analyses. Specifically, the P1 amplitude was corrected for the N1 amplitude (corrected P1 amplitude = P1 - N1 amplitude); the P1 latency was corrected for the N1 latency (corrected P1 latency = P1 - N1 latency); the N2 amplitude was corrected for the P1 amplitude (corrected N2 amplitude = N2 - P1 amplitude), and the N2 latency was corrected for the P1 latency (corrected N2 latency = N2 - P1 latency).

All VEPs were visually inspected to ensure that the automatically extracted values were correct and were adjusted if observable peaks occurred outside the automated window bounds. Participants were considered to have failed this visual inspection and were subsequently removed from the data set if their VEP did not produce three discernible peaks. VEP waveforms of included participants by timepoint are included in Figure 1E. XX infants provided usable VEP data at Visit 1, XX infants provided usable VEP data at Visit 2, and XX infants provided usable VEP data at Visit 3. There were no differences in EEG quality (i.e., number of trials collected, number/percent of trials retained, number/percent of channels retained overall, number/percent of channels retained in ROI) by time point (all $p>.05$).

Biospecimens and sequencing

Sample Collection

Stool samples were collected in the clinic by the research assistant directly from the diaper and transferred to the Zymo DNA/RNA Shield™ Fecal collection Tube (#R1101, Zymo Research Corp., Irvine, USA) and immediately frozen at -80 ˚C. Stool samples were not collected if the subject had taken antibiotics within the two weeks prior to sampling.

DNA Extraction

DNA extraction was performed at Medical Microbiology, University of Cape Town, South Africa from stool samples collected in DNA/RNA Shield™ Fecal collection tube using the Zymo Research Fecal DNA MiniPrep kit (# D4003, Zymo Research Corp., Irvine, USA) following manufacturer's protocol. To assess the extraction process's quality, ZymoBIOMICS® Microbial Community Standards (#D6300 and #D6310, Zymo Research Corp., Irvine, USA) were incorporated and subjected to the identical process as the stool samples. The DNA yield and purity were determined using the NanoDrop® ND -1000 (Nanodrop Technologies Inc. Wilmington, USA).

Sequencing

Shotgun metagenomic sequencing was performed on all samples at the Integrated Microbiome Research Resource (IMR, Dalhousie University, NS, Canada). A pooled library (max 96 samples per run) was prepared using the Illumina Nextera Flex Kit for MiSeq and NextSeq from 1 ng of each sample. Samples were then pooled onto a plate and sequenced on the Illumina NextSeq 2000 platform using 150+150 bp paired-end P3 cells, generating 24M million raw reads and 3.6 Gb of sequence per sample.

Statistics / computational analysis

Metagenome processing

Raw metagenomic sequence reads were processed using tools from the bioBakery as previously described (Bonham et al. 2023; Beghini et al. 2021). Briefly, KneadData v0.10.0 was used with default parameters to trim low-quality reads and remove human sequences (using reference database hg37). Next, MetaPhlAn v3.1.0 (using database mpa_v31_CHOCOPhlAn_201901) was used with default parameters to map microbial marker genes to generate taxonomic profiles. Taxonomic profiles and raw reads were passed to HUMAnN v3.7 to generate stratified functional profiles.

Microbial community analysis

Principal coordinates analysis was performed in the julia programming language (Bezanson et al. 2012) using the Microbiome.jl package (Bonham et al. 2021). Bray-Curtis dissimilarity (Distances.jl) was calculated across all pairs of samples, filtering for species-level classification. Classical multidimensional scaling was performed on the dissimilarity matrix (MultivariateStats.jl), and axes with negative eigenvalues were discarded.

Feature Set Enrichment Analysis (FSEA)

Potentially neuroactive genesets were extracted from Supplementary Dataset 1 from (Valles-Colomer et al. 2019). Gut-brain modules provide Kegg Orthologue IDs (KOs), which were mapped to UniRef90 IDs using the utility mapping file provided with HUMAnN v3.1. For each

stool / VEP pair, logistic regression (LR) was performed linking the presence of absence of that UniRef in a sample with each VEP feature (N1, P1, and N2 latencies and amplitudes), controlling for the age at which the stool sample was collected, the number of retained VEP trials, and the difference in age between the stool collection and VEP measurement. For concurrently collected stool and VEP comparisons (Figure 2), subjects whose stool collection and VEP measurements were more than 2 months apart were excluded.

(1) UniRef ~ vep + age_months + n_trials + age_diff

FSEA was performed on each geneset that had at least 5 members in each comparison group according to the procedure set out in Subramanian *et. al.* (2005)(Subramanian et al. 2005). Briefly, enrichment scores (ES) are calculated based on the rank-order of z-statistics from the LR for each UniRef. A permutation test was then performed where the ES for 5000 random samples of ranks of the same length as the gene set are calculated, and the pseudo-p value is the number fraction of permutations where the permutation ES has a greater absolute value than the true ES.

Benjamini-Hochberg FDR correction was performed separately on all concurrently tested geneset / VEP feature combinations, and all longitudinal geneset / VEP feature combinations. Corrected p-values (q values) less than 0.2 were considered statistically significant.

References

Aburto, María R., and John F. Cryan. 2024. “Gastrointestinal and Brain Barriers: Unlocking Gates of Communication across the Microbiota–Gut–Brain Axis.” *Nature Reviews Gastroenterology & Hepatology* 21 (4): 222–47. https://doi.org/10.1038/s41575-023-00890-0.

Agus, Allison, Julien Planchais, and Harry Sokol. 2018. “Gut Microbiota Regulation of Tryptophan Metabolism in Health and Disease.” *Cell Host & Microbe* 23 (6): 716–24. https://doi.org/10.1016/j.chom.2018.05.003.

Ahmed, Hany, Quentin Leyrolle, Ville Koistinen, Olli Kärkkäinen, Sophie Layé, Nathalie Delzenne, and Kati Hanhineva. 2022. “Microbiota-Derived Metabolites as Drivers of Gut–Brain Communication.” *Gut Microbes* 14 (1): 2102878. https://doi.org/10.1080/19490976.2022.2102878.

Ahrens, Angelica P., Tuulia Hyötyläinen, Joseph R. Petrone, Kajsa Igelström, Christian D. George, Timothy J. Garrett, Matej Orešič, Eric W. Triplett, and Johnny Ludvigsson. 2024. “Infant Microbes and Metabolites Point to Childhood Neurodevelopmental Disorders.” *Cell* 187 (8): 1853-1873.e15. https://doi.org/10.1016/j.cell.2024.02.035.

Bäckhed, Fredrik, Josefine Roswall, Yangqing Peng, Qiang Feng, Huijue Jia, Petia Kovatcheva-Datchary, Yin Li, et al. 2015. “Dynamics and Stabilization of the Human Gut Microbiome during the First Year of Life.” *Cell Host & Microbe* 17 (5): 690–703. https://doi.org/10.1016/j.chom.2015.04.004.

Baj, Andreina, Elisabetta Moro, Michela Bistoletti, Viviana Orlandi, Francesca Crema, and Cristina Giaroni. 2019. “Glutamatergic Signaling Along The Microbiota-Gut-Brain Axis.” *International Journal of Molecular Sciences* 20 (6): 1482. https://doi.org/10.3390/ijms20061482.

Beghini, Francesco, Lauren J McIver, Aitor Blanco-Míguez, Leonard Dubois, Francesco

Asnicar, Sagun Maharjan, Ana Mailyan, et al. 2021. “Integrating Taxonomic, Functional, and Strain-Level Profiling of Diverse Microbial Communities with bioBakery 3.” *Elife* 10 (May). https://doi.org/10.7554/eLife.65088.

Bezanson, Jeff, Stefan Karpinski, Viral B Shah, and Alan Edelman. 2012. “Julia: A Fast Dynamic Language for Technical Computing,” September. http://arxiv.org/abs/1209.5145.

Bonham, Kevin, Guilherme Fahur Bottino, Shelley Hoeft McCann, Jennifer Beauchemin, Elizabeth Weisse, Fatoumata Barry, Rosa Cano Lorente, et al. 2023. “Gut-Resident Microorganisms and Their Genes Are Associated with Cognition and Neuroanatomy in Children.” *Science Advances* 9 (51): eadi0497. https://doi.org/10.1126/sciadv.adi0497.

Bonham, Kevin, Annelle Kayisire, Anika Luo, and Vanja Klepac-Ceraj. 2021. “Microbiome.Jl and BiobakeryUtils.Jl - Julia Packages for Working with Microbial Community Data.” *Journal of Open Source Software* 6 (67): 3876. https://doi.org/10.21105/joss.03876.

Canipe, L. Grant, Michael Sioda, and Carol L. Cheatham. 2021. “Diversity of the Gut-Microbiome Related to Cognitive Behavioral Outcomes in Healthy Older Adults.” *Archives of Gerontology and Geriatrics* 96 (September):104464. https://doi.org/10.1016/j.archger.2021.104464.

Chen, Tong, Daisuke Noto, Yasunobu Hoshino, Miho Mizuno, and Sachiko Miyake. 2019. “Butyrate Suppresses Demyelination and Enhances Remyelination.” *Journal of Neuroinflammation* 16 (1): 165. https://doi.org/10.1186/s12974-019-1552-y.

Collins, Stephen M., Michael Surette, and Premysl Bercik. 2012. “The Interplay between the Intestinal Microbiota and the Brain.” *Nature Reviews Microbiology* 10 (11): 735–42. https://doi.org/10.1038/nrmicro2876.

Dalile, Boushra, Lukas Van Oudenhove, Bram Vervliet, and Kristin Verbeke. 2019. “The Role of Short-Chain Fatty Acids in Microbiota-Gut-Brain Communication” 16 (8): 461–78. https://doi.org/10.1038/s41575-019-0157-3.

Dean, Douglas C., Jonathan O’Muircheartaigh, Holly Dirks, Nicole Waskiewicz, Katie Lehman, Lindsay Walker, Michelle Han, and Sean C. L. Deoni. 2014. “Modeling Healthy Male White Matter and Myelin Development: 3 through 60 Months of Age.” *NeuroImage* 84 (January):742–52. https://doi.org/10.1016/j.neuroimage.2013.09.058.

Deen, Ben, Hilary Richardson, Daniel D. Dilks, Atsushi Takahashi, Boris Keil, Lawrence L. Wald, Nancy Kanwisher, and Rebecca Saxe. 2017. “Organization of High-Level Visual Cortex in Human Infants.” *Nature Communications* 8 (1): 13995. https://doi.org/10.1038/ncomms13995.

Dekkers, Koen F., Sergi Sayols-Baixeras, Gabriel Baldanzi, Christoph Nowak, Ulf Hammar, Diem Nguyen, Georgios Varotsis, et al. 2022. “An Online Atlas of Human Plasma Metabolite Signatures of Gut Microbiome Composition.” *Nature Communications* 13 (1): 5370. https://doi.org/10.1038/s41467-022-33050-0.

Deng, Kui, Jin-jian Xu, Luqi Shen, Hui Zhao, Wanglong Gou, Fengzhe Xu, Yuanqing Fu, et al. 2023. “Comparison of Fecal and Blood Metabolome Reveals Inconsistent Associations of the Gut Microbiota with Cardiometabolic Diseases.” *Nature Communications* 14 (1): 571. https://doi.org/10.1038/s41467-023-36256-y.

Ellis, Cameron T., Tristan S. Yates, Lena J. Skalaban, Vikranth R. Bejjanki, Michael J. Arcaro, and Nicholas B. Turk-Browne. 2021. “Retinotopic Organization of Visual Cortex in Human Infants.” *Neuron* 109 (16): 2616-2626.e6. https://doi.org/10.1016/j.neuron.2021.06.004.

Erny, Daniel, Nikolaos Dokalis, Charlotte Mezö, Angela Castoldi, Omar Mossad, Ori Staszewski, Maximilian Frosch, et al. 2021. “Microbiota-Derived Acetate Enables the Metabolic Fitness of the Brain Innate Immune System during Health and Disease.” *Cell Metabolism* 33 (11): 2260-2276.e7. https://doi.org/10.1016/j.cmet.2021.10.010.

Fagiolini, M., and T. K. Hensch. 2000. “Inhibitory Threshold for Critical-Period Activation in

543 Primary Visual Cortex." *Nature* 404 (6774): 183–86. https://doi.org/10.1038/35004582.
544 Filpa, Viviana, Elisabetta Moro, Marina Protasoni, Francesca Crema, Gianmario Frigo, and
545 Cristina Giaroni. 2016. "Role of Glutamatergic Neurotransmission in the Enteric Nervous
546 System and Brain-Gut Axis in Health and Disease." *Neuropharmacology* 111
547 (December):14–33. https://doi.org/10.1016/j.neuropharm.2016.08.024.
548 Gilbert, Jack A., Martin J. Blaser, J. Gregory Caporaso, Janet K. Jansson, Susan V. Lynch, and
549 Rob Knight. 2018. "Current Understanding of the Human Microbiome." *Nature Medicine*
550 24 (4): 392–400. https://doi.org/10.1038/nm.4517.
551 Hensch, Takao K., Michela Fagiolini, Nobuko Mataga, Michael P. Stryker, Steinunn
552 Baekkeskov, and Shera F. Kash. 1998. "Local GABA Circuit Control of Experience-
553 Dependent Plasticity in Developing Visual Cortex." *Science* 282 (5393): 1504–8.
554 https://doi.org/10.1126/science.282.5393.1504.
555 Janik, Rafal, Lynsie A. M. Thomason, Andrew M. Stanisz, Paul Forsythe, John Bienenstock,
556 and Greg J. Stanisz. 2016. "Magnetic Resonance Spectroscopy Reveals Oral
557 Lactobacillus Promotion of Increases in Brain GABA, N-Acetyl Aspartate and
558 Glutamate." *NeuroImage* 125 (January):988–95.
559 https://doi.org/10.1016/j.neuroimage.2015.11.018.
560 Kennedy, Elizabeth A., Katherine Y. King, and Megan T. Baldridge. 2018. "Mouse Microbiota
561 Models: Comparing Germ-Free Mice and Antibiotics Treatment as Tools for Modifying
562 Gut Bacteria." *Frontiers in Physiology* 9.
563 https://www.frontiersin.org/articles/10.3389/fphys.2018.01534.
564 Kiorpes, Lynne. 2015. "Visual Development in Primates: Neural Mechanisms and Critical
565 Periods." *Developmental Neurobiology* 75 (10): 1080–90.
566 https://doi.org/10.1002/dneu.22276.
567 Koenig, Jeremy E, Aymé Spor, Nicholas Scalfone, Ashwana D Fricker, Jesse Stombaugh, Rob
568 Knight, Largus T Angenent, and Ruth E Ley. 2011. "Succession of Microbial Consortia in
569 the Developing Infant Gut Microbiome." *Proceedings of the National Academy of*
570 *Sciences of the United States of America* 108 Suppl 1 (March):4578–85.
571 https://doi.org/10.1073/pnas.1000081107.
572 Li, Jianrong, Judith C. Lin, Hong Wang, James W. Peterson, Barbara C. Furie, Bruce Furie,
573 Sara L. Booth, Joseph J. Volpe, and Paul A. Rosenberg. 2003. "Novel Role of Vitamin K
574 in Preventing Oxidative Injury to Developing Oligodendrocytes and Neurons." *Journal of*
575 *Neuroscience* 23 (13): 5816–26. https://doi.org/10.1523/JNEUROSCI.23-13-
576 05816.2003.
577 Lippé, S, M-S Roy, C Perchet, and M Lassonde. 2007. "Electrophysiological Markers of
578 Visuocortical Development." *Cerebral Cortex* 17 (1): 100–107.
579 https://doi.org/10.1093/cercor/bhj130.
580 Lugo-Huitrón, Rafael, Perla Ugalde Muñiz, Benjamin Pineda, José Pedraza-Chaverrí, Camilo
581 Ríos, and Verónica Pérez-de la Cruz. 2013. "Quinolinic Acid: An Endogenous
582 Neurotoxin with Multiple Targets." *Oxidative Medicine and Cellular Longevity*
583 2013:104024. https://doi.org/10.1155/2013/104024.
584 Lupori, Leonardo, Sara Cornuti, Raffaele Mazziotti, Elisa Borghi, Emerenziana Ottaviano,
585 Michele Dei Cas, Giulia Sagona, Tommaso Pizzorusso, and Paola Tognini. 2022. "The
586 Gut Microbiota of Environmentally Enriched Mice Regulates Visual Cortical Plasticity."
587 *Cell Reports* 38 (2): 110212. https://doi.org/10.1016/j.celrep.2021.110212.
588 Meyer, Katie, Anju Lulla, Kunal Debroy, James M. Shikany, Kristine Yaffe, Osorio Meirelles, and
589 Lenore J. Launer. 2022. "Association of the Gut Microbiota With Cognitive Function in
590 Midlife." *JAMA Network Open* 5 (2): e2143941.
591 https://doi.org/10.1001/jamanetworkopen.2021.43941.
592 Monachino, A D, K L Lopez, L J Pierce, and L J Gabard-Durnam. 2022. "The HAPPE plus
593 Event-Related (HAPPE+ER) Software: A Standardized Preprocessing Pipeline for

Event-Related Potential Analyses." *Modeling Neural Development* 57 (101140): 101140. https://doi.org/10.1016/j.dcn.2022.101140.

Parker, Aimée, Sonia Fonseca, and Simon R. Carding. 2019. "Gut Microbes and Metabolites as Modulators of Blood-Brain Barrier Integrity and Brain Health." *Gut Microbes* 11 (2): 135–57. https://doi.org/10.1080/19490976.2019.1638722.

Rhee, Sang H., Charalabos Pothoulakis, and Emeran A. Mayer. 2009. "Principles and Clinical Implications of the Brain-Gut-Enteric Microbiota Axis." *Nature Reviews. Gastroenterology & Hepatology* 6 (5): 306–14. https://doi.org/10.1038/nrgastro.2009.35.

Subramanian, Aravind, Pablo Tamayo, Vamsi K. Mootha, Sayan Mukherjee, Benjamin L. Ebert, Michael A. Gillette, Amanda Paulovich, et al. 2005. "Gene Set Enrichment Analysis: A Knowledge-Based Approach for Interpreting Genome-Wide Expression Profiles." *Proceedings of the National Academy of Sciences* 102 (43): 15545–50. https://doi.org/10.1073/pnas.0506580102.

Takesian, Anne E., Luke J. Bogart, Jeff W. Lichtman, and Takao K. Hensch. 2018. "Inhibitory Circuit Gating of Auditory Critical-Period Plasticity." *Nature Neuroscience* 21 (2): 218–27. https://doi.org/10.1038/s41593-017-0064-2.

Tavares, Rejane G., Carla I. Tasca, Candice E. S. Santos, Moacir Wajner, Diogo O. Souza, and Carlos S. Dutra-Filho. 2000. "Quinolinic Acid Inhibits Glutamate Uptake into Synaptic Vesicles from Rat Brain." *NeuroReport* 11 (2): 249.

Valles-Colomer, Mireia, Gwen Falony, Youssef Darzi, Ettje F Tigchelaar, Jun Wang, Raul Y Tito, Carmen Schiweck, et al. 2019. "The Neuroactive Potential of the Human Gut Microbiota in Quality of Life and Depression." *Nature Microbiology* 4 (4): 623–32. https://doi.org/10.1038/s41564-018-0337-x.

Wymore Brand, Meghan, Michael J. Wannemuehler, Gregory J. Phillips, Alexandra Proctor, Anne-Marie Overstreet, Albert E. Jergens, Roger P. Orcutt, and James G. Fox. 2015. "The Altered Schaedler Flora: Continued Applications of a Defined Murine Microbial Community." *ILAR Journal* 56 (2): 169–78. https://doi.org/10.1093/ilar/ilv012.

Yassour, Moran, Tommi Vatanen, Heli Siljander, Anu-Maaria Hämäläinen, Taina Härkönen, Samppa J Ryhänen, Eric A Franzosa, et al. 2016. "Natural History of the Infant Gut Microbiome and Impact of Antibiotic Treatment on Bacterial Strain Diversity and Stability." *Science Translational Medicine* 8 (343): 343ra81. https://doi.org/10.1126/scitranslmed.aad0917.

Zieff, Michal R, Marlie Miles, Emmie Mbale, Emma Eastman, Lorna Ginnell, Steven C R Williams, Derek K Jones, et al. 2024. "Characterizing Developing Executive Functions in the First 1000 Days in South Africa and Malawi: The Khula Study." *Wellcome Open Research* 9 (March):157. https://doi.org/10.12688/wellcomeopenres.19638.1.